High Frequency CMOS *Gm-C* Bandpass Filter Design

Haijun LIN, Atsushi MOTOZAWA, Kazuya SHIMIZU,
Yousuke TAKAHASHI, Masafumi UEMORI,
Haruo KOBAYASHI, Tomoyuki TANABE, Nobukazu TAKAI, Hao SAN

Electronic Engineering Department, Gunma University

E-mail : lin@el.gunma-u.ac.jp, k_haruo@el.gunma-u.ac.jp

ABSTRACT

This paper describes design of a high-frequency high-Q second-order *Gm-C* bandpass filter based on Nauta's OTAs used for the RF sampling continuous-time bandpass $\Delta\Sigma$AD modulator. By using $0.25\mu m$ CMOS process, a *Gm-C* bandpass filter with center frequency of 1GHz, bandwidth of 33MHz and Q factor of 30 may be feasible. We also discuss its nonlinearity, noise and power issues.

Keywords: *CMOS, OTA, Gm-C Filter, Bandpass Delta-Sigma Modulator, RF Sampling*

1. Introduction

A high-frequency, low-power continuous-time bandpass $\Delta\Sigma$ AD has been investigated for portable communication system applications such as WLAN, cellular phone [1, 2, 3]. A G_m-C bandpass filter (BPF) can be used as a high-frequency, low-power bandpass filter inside such a $\Delta\Sigma$ AD modulator.

For our design target of a RF direct sampling bandpass $\Delta\Sigma$ modulator [1, 2], its center frequency f_c should be as high as several hundreds MHz or higher, since f_c=$2\pi g_m/C$ and C must be large enough for noise performance, the CMOS Operational Transconductance Amplifier (OTA) circuit has to have a large value of g_m with good high frequency characteristics. A suitable option of the OTA circuit with no internal nodes was presented by Nauta [5]. In this work, we will clarify high-frequency characterisitcs, Q, linearity, noise and power issues of a second-order bandpass filter as well as optimum Nauta's OTA circuit design and tuning circuit considering parasitics in $0.25\mu m$ CMOS process. We have confirmed its center frequency of 1GHz and Q of 30 by SPICE simulation with BSIM3v3 parameters.

2. Analysis of Nauta OTA circuit

Fig.1 shows a Nauta's OTA circuit [5, 6], where four inverters at the output provide both common mode stability and high differential mode output resistance. Since high-order poles are not introduced by the internal node parasitic capacitances, there an (almost) ideal integrator can be implemented; it is suitable for high frequency bandpass filter. By adjusting the power supply voltage Vdd' for Inv4, Inv5 in Fig.1, the output resistance can be made large and very high DC gain can be realized. For the OTA design, nonlinearity and noise issues are also important and we will discuss them in the followings.

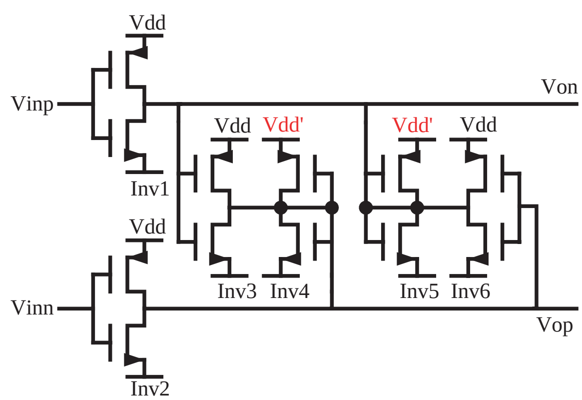

Fig. 1. Nauta OTA circuity.

2.1 Nonlinearity Analysis of Nauta OTA

A dominant source of Nauta OTA nonlinearity is mobility reduction due to vertical field and parasitic capacitance in high frequency region. Electron and hole mobilities in MOSFETs can be expressed as

$$\begin{aligned} \mu_n : &= \frac{\mu_{n0}}{1+\theta_n(V_{gsn}-V_{thn})} \\ \mu_p : &= \frac{\mu_{p0}}{1+\theta_p(V_{sgp}-|V_{thp}|)}. \end{aligned}$$

The output currents from core inverters in Nauta

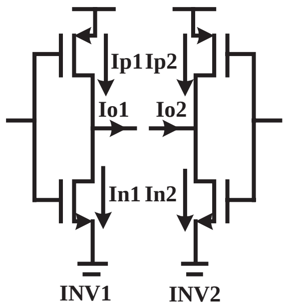

Fig. 2. Output currents of core inverters in Nauta OTA.

OTA (Fig.2) are given by

$$\begin{aligned} I_{od} &= I_{o1} - I_{o2} \\ &= (I_{n1} - I_{p1}) - (I_{n2} - I_{p2}) \\ &= (I_{n1} - I_{n2}) + (I_{p2} - I_{p1}). \end{aligned}$$

Using Taylor expansion, they are approximated by

$$\begin{aligned} I_{n1} - I_{n2} &\approx \frac{\beta_{0n} V_{on}(1 + \frac{1}{2}\theta_n V_{on})}{(1 + \theta_n V_{on})^2} \cdot V_{id} \\ &\quad - \frac{\theta_n \beta_{0n}}{2(1 + \theta_n V_{on})^4} \frac{1}{4} V_{id}^3. \\ I_{p2} - I_{p1} &\approx \frac{\beta_{0p} V_{op}(1 + \frac{1}{2}\theta_p V_{op})}{(1 + \theta_p V_{op})^2} \cdot V_{id} \\ &\quad - \frac{\theta_p \beta_{0p}}{2(1 + \theta_p V_{op})^4} \frac{1}{4} V_{id}^3. \end{aligned}$$

Here

$$\begin{aligned} V_{on} &= V_{cm} - V_{thn}, \quad V_{op} = V_{DD} - V_{cm} - |V_{thp}| \\ \beta_{0n} &= \mu_{n0} C_{ox} \frac{W_n}{L_n}, \quad \beta_{0p} = \mu_{p0} C_{ox} \frac{W_p}{L_p}. \end{aligned}$$

Now we have a differntial output current as $I_{od} \approx c_1 V_{id} + c_3 V_{id}^3$, and we assume that $\beta_{0n} \approx \beta_{0p} = \beta_0$, $V_{on} = V_{op} = V_o$, $c_1 \approx 2\beta_0 V_o$, $c_3 \approx -\frac{\beta_0}{8}(\theta_n + \theta_p)$, $g_m(V_{id}) = \frac{\delta I_{od}}{\delta V_{id}} = c_1 + 3c_3 V_{id}^2$. Then we have the third-order distortion of Nauta OTA as

$$\frac{c_3}{c_1} \approx -\frac{\theta_n + \theta_p}{16 V_o} = -\frac{\theta_n + \theta_p}{8(V_{DD} - |V_{thp}| - V_{thn})}. \quad (1)$$

2.2 Noise Analysis of Nauta OTA

In high frequency region, the dominant noise source is thermal noise from MOSFETs, and Fig.3 is a noise model of Nauta OTA. The output equivalent current noise for one inverter can be expressed as
$\overline{i_{inv}^2} = 4\gamma_n kT gm_n df + 4\gamma_p kT gm_p df$.
Here we assume that $gm_n = gm_p$, $\gamma_n = \gamma_p (= \gamma_{inv}$, noise factor), $gm_n + gm_p = gm_{inv}$. Then we have

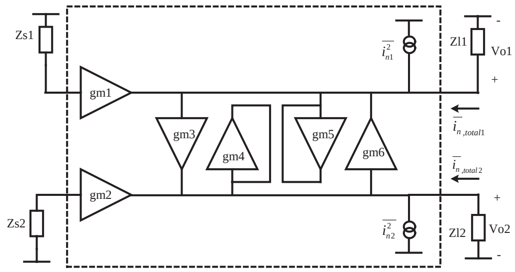

Fig. 3. Noise model of Nauta OTA.

the total output equivalent current noise as follows:

$$\overline{i_{nd}^2} = 4\gamma_{inv} kT df \sum_{i=1}^{6} gm_i \quad (2)$$

Considering the above-mentioned nonlinearity and noise performance, we have designed an OTA with 48dB DC gain (Fig.4 shows frequency characteristics of an integrator using this OTA).

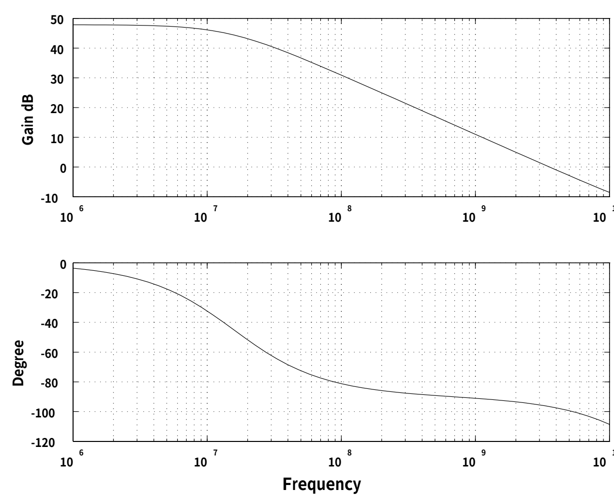

Fig. 4. Simulated gain and phase of a *Gm-C* integrator with a designed OTA.

3. Bandpass *Gm-C* Filter Design

Active and passive filters can be used for bandpass filter design. Active filters can be classified into active RC filters which use operational amplifiers, and *Gm-C* filters which use OTAs [3]. RC polyphase filters [7] and LCR filters are passive-type, and a passive LCR filter can be a model of a *Gm-C* filter where

L and R are equivalently realized by OTAs to save chip area. The *Gm-C* filter operates in open-loop which is suitable for high frequency operation, and g_m value can be adjusted automatically by an embedded tuning circuit. Our design target here is a *Gm-C* bandpass filter with the center frequency $f_c = 1$GHz, $Q = 30$ and $A_v(1GHz) = 20$dB.

3.1 Second-Order Bandpass Filter Design

Fig.5 shows a second-order *Gm-C* filter which models an LCR filter; g_{m1} is the input OTA while the inductor is equivalently made by two OTA cells (g_m) and a capacitor C_2, and a resistor is by an OTA (g_{m2}). Then its transfer function is given by

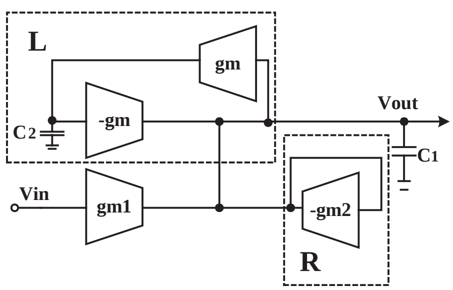

Fig. 5. *Gm-C* BPF configuration.

$$H(s) = \frac{V_{out}}{V_{in}} = \frac{\frac{g_{m1} s C_2}{g_m^2}}{\frac{s^2 C_1 C_2}{g_m^2} + \frac{g_{m2} s C_2}{g_m^2} + 1}. \qquad (3)$$

Here $\omega_0 = \frac{g_m}{\sqrt{C_1 C_2}}$, $Q = \frac{g_m}{g_{m2}} \cdot \frac{\sqrt{C_2}}{\sqrt{C_1}}$, $A = \frac{g_{m1}}{g_{m2}}$.

3.2 High Frequency Operation

For high frequency performance of the filter, parasitic capacitance effects cannot be ignored; the parasitic capacitances of OTA circuits used in the filter may be virtually magnified due to Miller effect. Assume that parasitic capacitances are concentrated at the input and output nodes of OTA circuits (Fig.6). Parasitic capacitances and capacitors C_1, C_2 of the bandpass filter determine its high frequency performance, and the whole capacitances $C_{\text{eff1}}, C_{\text{eff2}}$ are expressed as

$C_{\text{eff1}} \approx C_1 + C_{gs,gm} + C_{gs,gm2}$

$C_{\text{eff2}} \approx C_2 + C_{gs,gm}$.

The transfer function of the filter is given by

$$H(s) = \frac{\frac{g_{m1} s C_{\text{eff2}}}{g_m^2}}{\frac{s^2 C_{\text{eff1}} C_{\text{eff2}}}{g_m^2} + \frac{g_{m2} s C_{\text{eff2}}}{g_m^2} + 1}. \qquad (4)$$

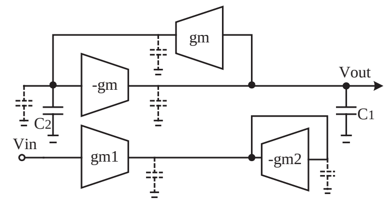

Fig. 6. *Gm-C* BPF with parasitic capacitances.

Thus parasitic capacitances deviate ω_0 and Q values as $\omega_0 = \frac{g_m}{\sqrt{C_{\text{eff1}} C_{\text{eff2}}}}$, $Q = \frac{g_m}{g_{m2}} \cdot \frac{\sqrt{C_{\text{eff2}}}}{\sqrt{C_{\text{eff1}}}}$. From our calculation, $C_{\text{eff1}} \approx 0.89pF$. $C_{\text{eff2}} \approx 0.87pF$, and we found that to achieve our design target, $g_m > 5.58mS$, $g_{min} > 1.86mS$, $g_{m2} > 0.186mS$ are necessary. Fig.7 shows SPICE simulated AC characteristics of a modeled LCR filter and our designed *Gm-C* filter with center frequency of 1GHz, voltage gain at 1GHz of 20dB and Q of 30. Fig.8 shows transient response of the designed bandpass filter.

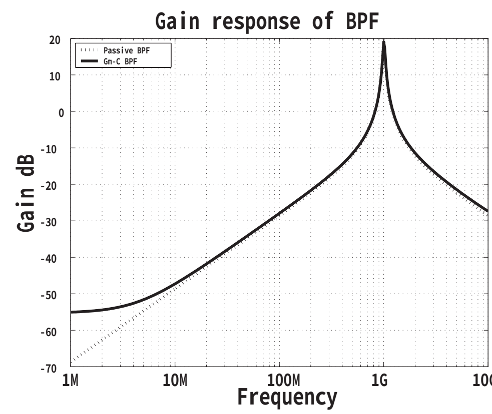

Fig. 7. AC analysis of a modeled LCR BPF and our designed *Gm-C* BPF filter.

3.3 Linearity Performance

Intermodulation distortion is the most important distortion factor for the bandpass filter, and the third-order intermodulation distortion (IM3) determines its linearity because the designed filter circuit is fully differential. When the input signal is given by

$$V_{in}(t) = A\cos(2\pi f_1 t) + A\cos(2\pi f_2 t),$$

we obtained $IM_3 \approx -41.2$dB for the input frequencies $f_1 = $1GHz, $f_2 = 1.01$GHz and the input ampli-

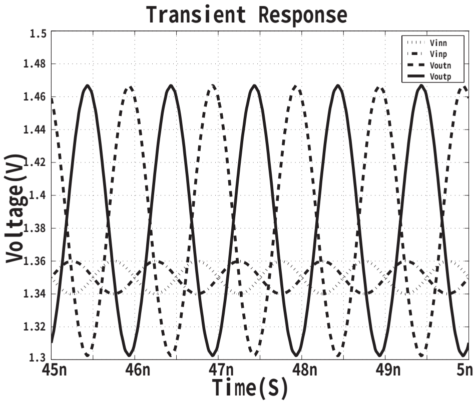

Fig. 8. Transient response of our *Gm-C* BPF.

tude $A = 20\text{mV}_{pp}$.

3.4 Noise Performance

The noise power of an RC circuit in whole band ($0 < f < \infty$) is known as kT/C, and we have found that of an LCR circuit is also kT/C in whole band.(which is independent of R, L values). Also the noise power of a bandpass filter in whole band is given by $Q \cdot kT/C$ [5]. However we do not have to consider the noise power in *whole* band, but we consider just the noise in the *signal* band ($f_0 - BW/2 < f < f_0 + BW/2$) and we have derived its expression.

Fig.9 shows the noise model of the bandpass filter, where $\overline{I_{nx}}$, ($x = 1, 2, 3, 4$) are the output noise currents. The output noise density can be obtained as follows:

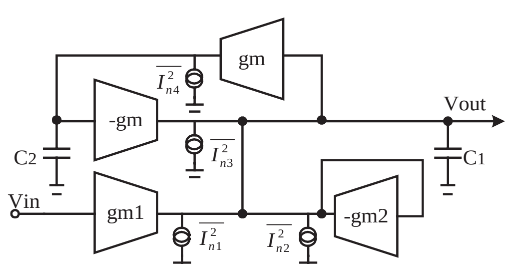

Fig. 9. Noise model of *Gm-C* BPF.

$$\overline{V^2_{In1out}} = \overline{I^2_{n1}}\left(\frac{\frac{sC_2}{g_m^2}}{1 + sC_2\frac{g_{m2}}{g_m^2} + s^2\frac{C_1C_2}{g_m^2}}\right)^2$$

$$\overline{V^2_{In2out}} = \overline{I^2_{n2}}\left(\frac{\frac{sC_2}{g_m^2}}{1 + sC_2\frac{g_{m2}}{g_m^2} + s^2\frac{C_1C_2}{g_m^2}}\right)^2$$

$$\overline{V^2_{In3out}} = \overline{I^2_{n3}}\left(\frac{\frac{sC_2}{g_m^2}}{1 + sC_2\frac{g_{m2}}{g_m^2} + s^2\frac{C_1C_2}{g_m^2}}\right)^2$$

$$\overline{V^2_{In4out}} = \overline{I^2_{n4}}\left(\frac{g_m}{sC_2}\right)^2\left(\frac{\frac{sC_2}{g_m^2}}{1 + sC_2\frac{g_{m2}}{g_m^2} + s^2\frac{C_1C_2}{g_m^2}}\right)^2.$$

For transfer function expressed by eq.(3),then the input equivalent noise power spectral density can be written as

$$\overline{V^2_{in}} = \frac{1}{g^2_{m1}}[\overline{I^2_{n1}} + \overline{I^2_{n2}} + \overline{I^2_{n3}} + \overline{I^2_{n4}}(\frac{g_m}{sC_2})^2]. \quad (5)$$

In high frequency region, we consider only thermal noise and we assume that $\overline{I_{nx}}$, $x = 1, 2, 3, 4$ are independent of frequency. Then the input equivalent noise in the signal band ($f_0 - BW/2 < f < f_0 + BW/2$) can be written as

$$\text{Noise}^2_{rms} = \int_{f_0-BW/2}^{f_0+BW/2} \text{Noise}^2_{dens} df.$$

Here, Noise^2_{rms} is the input equivalent noise power spectral density. Note that output noise current can be expressed as $\overline{I^2_{nx}} = 4\gamma kT g_{mi}$ ($x = 1, 2, 3, 4$, $g_{mi} = g_m, g_{m1}, g_{m2}$), where $\gamma = \frac{2}{3}$ is a noise factor of g_m cell.which will be much higher for short channel device. Then the input equivalent noise of this filter is given by

$$\begin{aligned}\text{Noise}^2_{rms} = \; & 4\gamma kT\tfrac{BW}{g_{m1}}[1 + \tfrac{g_{m2}}{g_{m1}} + \tfrac{g_m}{g_{m1}} \\ & + \tfrac{1}{4f_0^2 - BW^2}\tfrac{g_m}{g_{m1}}(\tfrac{g_m}{\pi C_2})^2].\end{aligned}$$

From eq. (3)

$$\frac{g_{m2}}{g_{m1}} = \frac{1}{A}$$

$$\frac{g_m}{q_{m1}} = \frac{Q}{A}\sqrt{\frac{C_2}{C_1}}$$

$$(\frac{g_m}{C_2})^2 = (\omega_0\sqrt{\frac{C_1}{C_2}})^2$$

Input equivalent noise in the signal band can be written as

$$\begin{aligned}\text{Noise}^2_{rms} = \; & \tfrac{8}{3}\gamma kT\tfrac{BW}{g_{m1}}[1 + \tfrac{1}{A} + \tfrac{Q}{A}\sqrt{\tfrac{C_2}{C_1}} \\ & + \tfrac{1}{4f_0^2 - BW^2}\tfrac{Q}{A}\tfrac{\omega_0^2}{\pi^2}\sqrt{\tfrac{C_1}{C_2}}].\end{aligned}$$

Since $BW << f_0$ in this work, the equation can be approximated as

$$\text{Noise}_{rms}^2 \approx \frac{4}{3}\gamma kT\frac{BW}{g_{m1}}[1+\frac{1}{A}+\frac{Q}{A}\frac{C_1+C_2}{\sqrt{C_1C_2}}]. \quad (6)$$

We see from eq.(6) that as g_{m1} increases, noise decreases and gain (A) increases. Note that increase of g_{m1} leads to increase of power; noise and power are trade-off. Also remark that if a high Q filter is required, it suffers from noise increase. In this work, we obtain the output noise density of $17.2\frac{nV}{\sqrt{Hz}}$ from SPICE simulation, where we replace C_1, C_2 with $C_{\text{eff}1}$, $C_{\text{eff}2}$ respectively.

3.5 Tuning of Center Frequency and Q

On-chip *Gm-C* bandpass filter requires tuning circuit for its center frequency and Q value to absorb process variation, supply voltage change and temperature change. In this work, we use PLL for center frequency tuning and Modified-LMS topology for Q tuning.

Fig.10 shows the whole tuning circuit for the center frequency and Q. Since tuning of the center frequency and that of Q may interact each other when both tunings operate simultaneously, only one tuning operates at one time (first center frequency tuning, then Q tuning are performed). Fig.11 and Fig.12 show the simulation result of a bandpass filter after tuning where 1% mismatch of MOSFTEs is included.

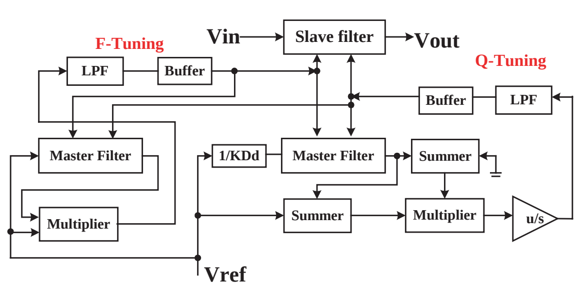

Fig. 10. Tunning circuit for center frequency and Q of our *Gm-C* BPF.

3.6 Whole G_m-C Bandpass Filter

Table 1 shows the SPICE simulation results of our whole *Gm-C* bandpass filter.

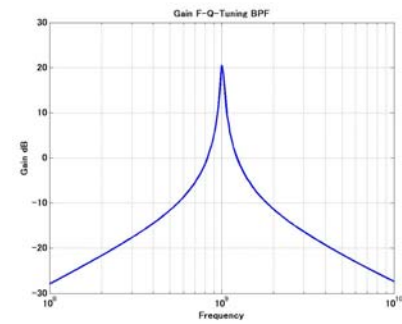

Fig. 11. Simulated gain characteristics of our *Gm-C* BPF after tuning.

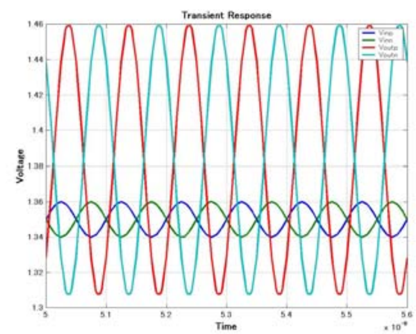

Fig. 12. Simulated transient response of our *Gm-C* BPF after tuning.

Table.1 Characteristics of $2nd$ order Gm-C bandpass filter

Process	$0.25\mu m$ CMOS
Filter Type	2nd-order bandpass
Power Supply	2.7V(V_{dd}), 2.85V(V'_{dd})
Power Conception	$<$ 50mW
PSRR	47.4dB
Center Frequency	1.0GHz
Passband Width	33MHz
Q-Factor	30
Passband Gain	19dB
Group Delay	4.57nS
Output Noise Density	$17.2nV/\sqrt{Hz}$
Noise(950MHz − 1.05GHz)	171.6μV$_{rms}$
IM$_3$	−41.2dB

4. Conclusion

We have shown the feasibility of a very high frequency CMOS *Gm-C* bandpass filter for an RF sampling continuous-time bandpass $\Delta\Sigma$ modulator. Usually we use an LCR filter to implement a very high frequency bandpass filter on CMOS IC, but it is area consuming and hence costly. We have investigated to replace passive components with active ones in a very high frequency filter where nonlinearity, noise and power issues should be taken care of. We have shown by simulation with 0.25μm CMOS BSIM3v3 parameters that by use of Nauta OTS circuit a bandpass filter with center frequency of 1GHz and Q of 30 would be feasible. As a next step, we will realize this filter as a real chip.

Acknowledgement

We would like to thank Pascal Ro Le, K. Iizuka, M. Miyamoto, M. Morimura and K. Wilkinson for valuable discussions.

References

[1] M. Uemori, H. Kobayashi, T. Ichikawa, A. Wada, K. Mashiko, T. Tsukada, M. Motta, " High-Speed Continuous-Time Subsampling Bandpass $\Delta\,\Sigma$ AD Modulator Architecture, "*IEICE Trans. Fundamentals*, E89-A, no.4, pp.916-923 (April 2006).

[2] A. Motozawa, K. Shimizu, M. Uemori, P. Lo Re, Y. Takahashi, K. Iizuka, H. Kobayashi, H. San, N. Takai, N. Okamoto, S. Nishida, " Design Methodology of Continuous-Time Bandpass $\Delta\Sigma$ Modulators for RF Sampling, "*The 20th Workshop on Circuits and Systems in Karuizawa*, pp.81-86 (April 2007).

[3] L. Breems, R. Rutten, R. Veldhoven, G. Weide, H. Termeer "A 56mW CT Quadrature Cascaded SD Modulator with 77dB DR in a NZIF 20MHz Band," *ISSCC Digest of Technical Papers,* (Feb. 2007).

[4] S. Dosho, T. Morie, H. Fujiyama, "A 200MHz Seventh-Order Equiripple Continuous-Time Filter by Design of Nonlienarity Suppression in 0.25μm CMOS Process," *IEEE Journal of Solid-State Circuits*, vol.37, no.5, pp.559-565 (May 2002).

[5] B. Nauta, "A CMOS Transconductance-C Filter Technique for Very High-Frequencies," *IEEE Journal of Solid-State Circuits*, vol.27, no.2, pp.142-153 (Feb. 1992).

[6] K. Komoriyama, E. Yoshida, M. Yashiki, H. Tanimoto, " A Very Wideband Fully Balanced Active RC Polyphase Filter Based on CMOS Inverters in 0.18um CMOS Technology," *Tech. Digest of VLSI Circuit Symp.* pp.98-99, Kyoto (June, 2007).

[7] F. Behbahani, Y. Kishigami, J. Leete and A. A. Abidi, "CMOS Mixers and Polyphase Filters for Large Image Rejection," *IEEE J. Solid-State Circuits,* vol.36, no.6, pp.873-887 (June 2001).

[8] P.Kallam, Edgar, A. Karsiliker, "An Enhanced Adaptive Q-Tuning Scheme for a 100-M Fully Symmetric OTA-Based Bandpass Filter" *IEEE J.Solid-state Circuits.* vol.38, no.6, pp.585-593 (Apr. 2003).